Icarus 243 (2014) 208–221

Contents lists available at ScienceDirect

Icarus

journal homepage: www.elsevier.com/locate/icarus

Quantitative analysis of the morphology of martian gullies and insights into their formation

Z. Yue [a], W. Hu [b], B. Liu [a], Y. Liu [a], X. Sun [a], Q. Zhao [a], K. Di [a,*]

[a] State Key Laboratory of Remote Sensing Science, Institute of Remote Sensing and Digital Earth Chinese Academy of Sciences, Beijing 100101, China
[b] IoT Perception Mine Research Center, China University of Mining and Technology, Xuzhou 221008, China

ARTICLE INFO

Article history:
Received 8 June 2013
Revised 17 June 2014
Accepted 18 August 2014
Available online 1 September 2014

Keywords:
Earth
Mars, surface
Geological processes

ABSTRACT

The process of formation of observed geologically recent gully features on Mars has remained a topic of intense debate since their discovery. In this study, we performed quantitative morphological analysis on certain parameters of gullies from different settings, such as crater walls, terraces, and sand dunes, on the martian surface in addition to the Meteor and Xiuyan craters on the Earth. The morphometric parameters were measured for cross profiles, which were extracted along each gully at certain intervals. Some interesting relationships among the parameters were determined, which could provide us a comprehensive understanding of the morphologies of the gullies'. The results show that strong correlations exist among those parameters, and the gullies are morphometrically similar, except for a scale difference in different geologic settings. The morphometric similarity implies that they were probably formed by some common processes. On the other hand, the morphometric differences indicate that the processes may have played different roles in the formation of the gullies. The formation of gullies on the Earth crater walls was heavily affected by surface flow and slippage, and pre-existing fractures and faults were also very influential in their formation. We propose that gullies in martian crater walls and terraces should have a similar formation mechanism, and they can probably account for most of gullies appearing on crater walls. The morphometric differences between the gullies in sand dunes and other gully types are probably a result of the disparity in lithological settings, which have significant influence on erosion ability even for the same agents.

1. Introduction

Gullies are a type of young phenomenon on the martian surface, and were first found by the Mars Orbiter Camera (MOC) on board the Mars Global Surveyor (MGS) in 2000 (Malin and Edgett, 2000). In the earlier study, most of the gullies were found exposed on crater walls or terraces (Fig. 1A and B), and they can be observed in all types of substrate (layered, massive, shattered, and rubble) (Treiman, 2003). Generally, they are composed of an alcove, a channel, and an apron, although not as distinctly in some areas as in others. The alcove is a theater-shaped wide region originating within the upper one-third of the slope encompassing the gully (Heldmann and Mellon, 2004). In some cases, the alcove may be filled by finer grains with a smoother texture relative to the surrounding material (Arfstrom, 2002), or may be very indistinct. If present, the alcove tapers downward to form the channel, which is often the primary part of many gullies. Channels appear incised into the slope surface, having steep walls with a distinctive V-shaped cross section (Malin and Edgett, 2000). Most of the channels are sinuous probably in response to topographic variations or the instability of certain type of flow (Mangold et al., 2010), and they often become narrower and shallower downslope. In addition, they often appear in polygonally patterned ground where the alcove and channel exist (Levy et al., 2009). Gullies can terminate with depositional aprons of variable sizes, which typically have a triangular shape and broaden downslope. The apron structure is sometimes incised by the channel (Fig. 1), and they can be composed of distinct lobe contacts, indicating that gullies are formed in several stages (e.g., Schon et al., 2009). The latitudinal distribution of such gullies shows the greatest concentration in the mid-latitudes in each hemisphere. In the southern hemisphere, the number of gully systems steadily declines poleward from 30°S with the minimum value occurring between 60°S and 63°S, and then rises again poleward from 63°S (Heldmann and Mellon, 2004). Most gullies in the 30–45°S latitude band occur on slopes below the angle of reposes, and the slopes are generally between

* Corresponding author. Present address: No. 20 Datun Road, Chaoyang District, Beijing 100101, China.
E-mail address: kcdi@irsa.ac.cn (K. Di).

http://dx.doi.org/10.1016/j.icarus.2014.08.028
0019-1035/

20° and 30° (Dickson et al., 2007). Heldmann and Mellon (2004) also showed that gully channel length generally decreases as the latitude increases (i.e., toward the South Pole). Gullies can occur on all orientations of slopes, and the poleward preference of gullies at any latitude should not be overemphasized (Heldmann and Mellon, 2004; Balme et al., 2006). In the northern hemisphere, the number of gully systems increases between 30°N and 45°N and then tends to taper off at higher latitudes (Heldmann et al., 2007), or most of the gullies are concentrated in the 30–55°N band (Bridges and Lackner, 2006; Kneissl et al., 2010). In addition, the most impressive feature is that gullies within the 30–35°N band exhibit a transitional morphology between dry and fluid-like features (Bridges and Lackner, 2006). Although gullies can occur in a wide range of latitudes, they are usually concentrated in several preferred locations such as Acidalia Planitia (45°N, 330°E), Utopia Planitia (40°N, 110°E), Dao Vallis (35°S, 30°E), the south polar pits (72°S, ~0°E), and the chaotic terrain north of Terra Sirenum (35°S, 190°E) (Heldmann and Mellon, 2004; Kneissl et al., 2010). The regionally clustered distribution of gullies may show that latitude alone cannot be considered responsible for their global distribution, and additional factors (e.g., elevation, slope, lithology, local climate/weather regime, and/or any combination of these) that vary regionally, may play important roles in determining the origin of gullies (Bleamaster and Crown, 2005).

The other type of unusual gullies on martian surface was reported in late time, mostly appeared on sand dunes, and has relatively longer incised channels (Costard et al., 2002; Mangold et al., 2003; Reiss and Jaumann, 2003). Those dune gullies, also called linear gullies (Dundas et al., 2012), have an unusual form that mostly consist of a long sinuous channel or trough, usually with terminal pits, but with minimal alcoves and depositional aprons (Fig. 1C). (Note that gullies similar to those in crater walls with obvious aprons and alcoves can also appear in sand dunes, and linear gullies also exist in crater walls, if there is sufficient accumulation of soft soil.) Some channels are connected with branching track, as in terrestrial channel networks, over hillslopes; however, few channels are connected together in the lower part. Most of the channels are accompanied by symmetric levees, which are especially visible in the terminal parts of the linear gullies (Mangold et al., 2003). All the linear gullies are located only in several dune fields inside large craters, the latitudinal distribution of which, from 45°S to 55°S, is also consistent with that of gullies in crater walls (Mangold et al., 2003; Reiss and Jaumann, 2003).

Gullies are very young in geologic time because of their fresh-looking appearance and the superposition of only a few impact craters (Malin and Edgett, 2000). Reiss et al. (2004) derived an absolute age of at most 3 Ma; however, they might be younger than 300,000 years from crater counts on overlaid dunes. Schon et al. (2009) studied a single well-developed gully system with secondary craters on one part of its depositional lobes in eastern Promethei Terra (~35°S, 131°E), and dated the gully as ca. 1.25 Ma by tracing back to the primary crater. Linear gullies on sand dunes are probably even younger because of the preservation of fresh-appearing erosion tracks and the absence of craters superposed on the dune surfaces on which they are situated, and estimated age upper limits are in the range of 100–10,000 years with an uncertainty factor of two (Reiss and Jaumann, 2003). However, the two categories of gullies are still active today, which has been verified by repeated observations from High Resolution Imaging Science Experiment (HiRISE) images (Diniega et al., 2010; Reiss et al., 2010). Dundas et al. (2012) summarized the activities of the gullies at 12 sites, focusing on the southern hemisphere, and found that the activities related to linear gullies mostly involved the appearance of meter-scale blocks in the channels and dark flows around the upper alcoves and channels. Gully activities of gullies on crater walls are much more remarkable, including meter-scale channel widening, movement of meter-scale boulders, and deposition of decameter-scale mounds of material (Diniega et al., 2011; Dundas et al., 2012). However, it is significant that most of the activities that are directly related to the gullies themselves occurred in sand dunes or soft soils, and the gullies may be linear or non-linear.

Numerous mechanisms have been proposed for martian gully formation, and earlier hypotheses were mainly inferred from the morphology and martian climatic conditions. These hypotheses can be divided into three broad categories (Schon et al., 2009): entirely dry mechanisms, underground wet mechanisms, and surficial wet mechanisms. The first category mainly refers to dry mass wasting of fine-grained materials (Treiman, 2003), and the numerical flow modeling results by Pelletier et al. (2008) also favor dry granular flows, although the presence of liquid water in these flow events cannot be ruled out. The underground wet mechanisms involve hypotheses on the release of groundwater (Malin and Edgett, 2000; Mellon and Phillips, 2001) and liquid CO_2 (Musselwhite et al., 2001), which could be liquefied at some depth under the overburden pressure. Finally, the surficial wet

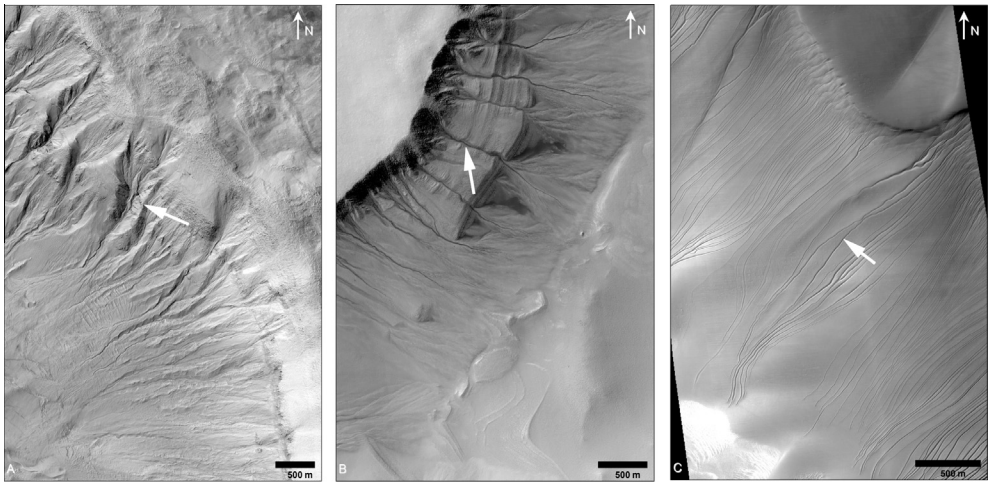

Fig. 1. Examples of martian gullies, indicated by the white arrows pointing respectively to a crater wall (A, HiRISE RED channel, subset of PSP_005943_1380), a terrace (B, HiRISE RED channel, subset of ESP_013585_1115), and sand dunes (C, HiRISE RED channel, subset of PSP_007018_1255).

mechanisms involve melting of shallow ground ice (Costard et al., 2002; Védie et al., 2008) and snowmelt (Christensen, 2003; Head et al., 2008). At the time of finding of the linear gullies, their formation was usually explained as being the result of rapid debris flows from melting of a surface layer of interstitial ice within dune deposits to a depth of several centimeters (e.g., Mangold et al. 2003; Reiss and Jaumann, 2003; Miyamoto et al., 2004). Since the discovery that the gullies' activities are ongoing, much attention has been paid to the current martian surface conditions favorable for the formation of gullies, and the significance of CO_2 was again raised. For example, Dundas et al. (2012) reported that most significant morphological changes are strongly associated with seasonal CO_2 frost and defrosting activity, and Diniega et al. (2013) proposed that blocks of CO_2 ice break from over-steepened cornices as sublimation processes destabilize the surface in the spring, and these blocks move downslope, carving out levéed grooves of relatively uniform width and forming terminal pits. There are many other studies supporting this idea (e.g., Hoffman, 2002; Diniega et al., 2010; Dundas et al., 2010), although there is also the objection that new alcoves and fans occur prior to CO_2 deposition (Horgan and Bell, 2012). However, there are still some interpretations that the changes in the linear gullies can be best explained by transient melting of small amounts of H_2O–ice triggering slurry flows consisting of sand mixed with liquid water (e.g., Reiss et al., 2010). In addition, we find that there are obvious differences (e.g., the sinuosity of the channels and the terminal pit morphology) between tracks from the movement of CO_2 ice blocks and linear gullies on sand dunes, although we cannot exclude a role for CO_2 in the formation of the gullies. In addition, the evaporation of CO_2 frost might also contribute to the transformation of martian gullies after they were formed, but there is no direct evidence that gullies were formed through this process. The complete absence of gullies in the equatorial region of Mars, the frequent occurrence of gullies in slopes well below the angle of repose (Dickson et al., 2007), and the lobate deposits in Protonilus Mensae (Levy et al., 2010), also seem difficult to reconcile with entirely dry mechanisms, and the wet mechanisms are still attractive. Considering the ongoing activities could occur both in linear and non-linear gullies, the occurrence of non-linear gullies on sand dunes, and the general consistency in distribution and source elevation (Dickson et al., 2007; Mangold et al., 2010), the two categories of gullies could possibly have been formed by a similar process except that the local lithological settings leads to the morphological difference.

An important issue for the wet mechanisms is the stability of liquid water and CO_2 during gullies' formation, which is probably from the most recent geologic time to present as we have addressed. On the suitability of martian present climate to the existence of liquid water, earlier models usually gave a negative result (e.g., Ingersoll, 1970). However, recently much more studies combing new observations support that liquid water could exist under present martian climates. For example, Lobitz et al. (2001) combined pressure and temperature data from the Viking mission with Mars Orbital Laser Altimeter (MOLA) data to show that liquid water would be stable over larger portions of the martian surface than was previously thought. Heldmann et al. (2007) found that, in the northern hemisphere, 95% of the gully alcove bases with adequate data coverage lie at depths at which the subsurface temperatures are greater than 273 K, 5% of the alcove bases lie within the solid water regime with the thermal conductivities derived from TES measurements as well as the modeled surface temperatures, and they are outside the temperature–pressure phase stability of liquid CO_2. The situation is similar in the southern hemisphere: 79% of the gully alcove bases lie at depths where subsurface temperatures are greater than 273 K, 21% of the alcove bases lie within the solid water regime, and most of the gully alcoves lie outside the temperature–pressure phase stability of liquid CO_2 (Heldmann and Mellon, 2004). Recent models of a validated general circulation by Haberle et al. (2001), and local heat transport on Mars by Hecht (2002), have also shown that liquid water can exist on present-day Mars for brief periods at optimal locations. In addition, thin liquid films of interfacial water can also play a role in rheological processes (Moehlmann, 2008; Kereszturi et al., 2009; Kossacki and Markiewicz, 2010), which provides a possible formation process of martian gullies by water. Because gullies have existed for a short interval in martian surface, many climate models have been devised to analyze whether martian past climate conditions were favorable to gullies' formation. For example, through General Circulation Model, Mischna et al. (2003) concluded that under past climate conditions there may have been centimeters of seasonal mid-latitude snowfall. Christensen (2003) showed that water-rich snow could be transported from the poles to mid-latitudes during periods of high obliquity within the past 10^5–10^6 years. Williams et al. (2009) also hypothesized that during past epochs of high obliquity the seasonal snowfields could exist at mid-latitudes, and they would be melted to produce surface debris flows in springtime to form the gullies.

Gullies appeared on the Earth too, and they also exhibit a similar morphology to those in martian crater walls or terraces, which makes it possible for us to analyze the formation mechanism of the martian gullies through their counterparts on the Earth. Reiss et al. (2011) studied the morphology of gullies on Svalbard (an archipelago in the Arctic Ocean), and concluded that gullies formed by debris flows would have levées, lobes, snouts, and debris plugs. Hobbs et al. (2014) conducted survey and remote sensing analysis of semiarid gullies, and found that the gullies would have different morphologies depending on the erosion agencies. For example, gullies that are topographically constrained to V-shaped channels and terminate in fluidized depositional aprons could be formed by water flow erosion (Hobbs et al., 2014). As the majority of martian gullies are located in crater walls, comparison of martian gullies with terrestrial analogs in crater walls can be an effective method for gaining an understanding of the formation of gullies on the martian surface. Kumar et al. (2010) expanded on observations of the Meteor crater interior and gullies, including sedimentary bedrock exposures on erosional scarps, talus deposits, and alluvial deposits, to document the distribution of gullies in the entire interior wall. This type of observation and comparison can provide very important insights into the nature of crater walls and the formation of overlying gullies. For example, the existence of abundant fractures and faults in a crater environment should be considered in genetic models of the formation of martian gullies (Kumar et al., 2010). Wang et al. (2013) found that most of the fractures along the inner wall of the Xiuyan crater are radial. The crater is located in metamorphic bedrock, and many of the fractures have developed into valleys extending hundreds of meters from the top of the rim to the floor of the crater. Observations of the Xiuyan crater have also shown that the fractures are critical for the formation of the valleys, and they are a type of tectonic characteristic related to impact upon the bedrock of the crater wall (Wang et al., 2013). In addition, a borehole has been drilled at the center of the Xiuyan crater, and the lacustrine sediments present in the stratigraphic column (Chen et al., 2010) clearly show that precipitation was involved in the formation of the gullies on the crater wall.

In this study, we studied the gullies in Xiuyan and Meteor craters on the Earth, and made a detailed morphometric comparison with gullies in various geologic environments of the crater wall, terrace and sand dunes on the martian surface. The morphometric parameters used in the study include basic information on the depth d, the width w, the length L, the derived sinuosity index S, and the slope s. Length represents the distances the material responsible for gullies' formation has traveled across the martian surface, and the longer gullies may indicate a greater degree of

gully activity (Heldmann and Mellon, 2004). Width and depth are the other two important basic indices in that they not only reflect the erosion ability laterally and vertically of the source agent, but they can also be used to estimate the gullies' volume by combing the length and then to infer the erosive power of gullies (Hobbs et al., 2014). Slope of gullies' cross-section can be used to infer the shape of gully cross profiles, which contribute to differentiate dry mass wasting and fluid-based processes (Hobbs et al., 2013). Sinuosity could be generated from topographic variations such as obstacles, roughness, or slope changes, while the source agent(s) of gullies may play much more effect (Mangold et al., 2010). Although some parameters have been used in previous studies of gullies, our study, however, focuses on the detailed morphometric information instead of the entire gully. For example, the sinuosity index S is usually calculated as the ratio between the total channel length and the straight line from the top to the bottom of each channel (e.g., Mangold et al., 2010). In contrast, we adopt a different strategy by slicing each gully into many cross-sections and calculating the sinuosity index S for each gully section from the top. Therefore, there are many values of the sinuosity index S for each gully, which can describe the morphometric characteristics of the gullies in great detail. We further tried to find correlations among the above parameters or their ratios (used to remove the influence of the magnitude), which would be useful in analyzing the formation of the gullies. In addition, the ratios of and the relationships between the parameters could also remove the influence of the geologic backgrounds at least to a certain extent. Soukhovitskaya and Manga (2006) employed a similar strategy by comparing the power–law relationships between the volume and the runout distance of landslides on Earth with those in Valles Marineris to conclude that water did not significantly influence the formation of landslides in Valles Marineris, which indicates that these types of analyses and comparisons can give some insights into the formation of gullies on Mars. Glines and Gulick (2014) also supported the idea that a gully formed by liquid flowing water at the surface or by other processes such as the sublimation of CO_2 or dry wall slumping events could be distinguished by comparing and contrasting local gullies.

2. Data

2.1. HiRISE images and derived digital terrain models

HiRISE (High Resolution Imaging Science Experiment) is a CCD (Charge-Coupled Device) camera onboard the MRO (Mars Reconnaissance Orbiter) which was launched on August, 2005. The HiRISE camera has a high SNR (Signal Noise Ratio), a large image size, and high resolution (McEwen et al., 2007). The focal plane contains a total of 14 CCD arrays, each of which operates as a 2048-pixel-wide line detector to build up an image in pushbroom mode, with up to 128 lines of time delay and integration (TDI) to ensure a high SNR. Ten of the detectors operating only in red wavelengths provide continuous coverage of a swath 20,048 pixels wide with slightly overlap in the cross-track direction (Kirk et al., 2008). The wide image from the red detectors is of the greatest utility for stereo analysis, provided at least two images of the same area on the ground are taken from different look angles. After interior orientation and corresponding point matching of HiRISE stereo images, a digital terrain model (DTM) of the martian surface can be derived using the method of photogrammetry, provided that the exterior orientation elements are available, which can usually be found in the SPICE kernel. Generating DTM from HiRISE stereo images is complex and time-consuming work; fortunately, some DTM products have been released by the HiRISE Operations Center (http://hirise.lpl.arizona.edu/), and the data used in the study are summarized in Table 1.

2.2. ZiYuan-3 satellite images and DEM in the Xiuyan crater

Xiuyan crater, located at 40.37°N, 123.46°E, is the first identified crater in the northern part of the Liaodong Peninsula of northern China. The diameter of the crater is about 1.8 km, and the maximum rim elevation above the present crater floor is 200 m (Chen et al., 2010). The crater rim is heavily eroded and many wide gullies are distributed radially (Fig. 2A). The ZY-3 (ZiYuan-3) surveying satellite is the first civilian high-resolution stereo mapping satellite of China. An optical panchromatic camera with a resulting image resolution of about 2.1 m was onboard. The camera operates in pushbroom mode, and time delay and integration (TDI) technology was used to ensure a high SNR, even in the shadow area (Tang et al., 2012). In this study, we acquired forward-, nadir- and backward-looking ZY-3 images covering the Xiuyan crater with associated rational polynomial coefficients (RPC). After block adjustment, dense image matching, and grid interpolation, a 10 m resolution digital elevation model (DEM) of the Xiuyan crater was obtained.

2.3. Meteor crater images and DEM from LiDAR

Meteor crater (aka Barringer crater) is the first identified impact crater on the Earth, and it has been extensively studied. There are also many gullies along the Meteor crater wall (Fig. 2B), which have been compared with their counterparts on the martian surface (Kumar et al., 2010). In the study, orthographic images from the USGS (United States Geological Survey) National Map Viewer along with airborne LiDAR DEM of Meteor crater were used to analyze the topographic characteristics of the gullies along the crater wall. The data can be downloaded through the website for the Meteor crater Map Package (http://www.lpi.usra.edu/publications/books/barringer_crater_guidebook/ArcGis/). The LiDAR data were acquired in March 2010 by the NCALM (National Center for Airborne Laser Mapping). The crater rim, walls, and interior were surveyed with a point density of 5 pts/m^2, while the surrounding terrain was surveyed with a point density of 8 pts/m^2, at a flight altitude of 600 m. This DEM product was generated from these point cloud data and has a resolution of 1 m, as used in the study (Brown et al., 2008). The orthographic image used in the study has been orthorectified and resampled to a spatial resolution of 1 m, which makes it completely matched with the DEM above.

3. Methodology

3.1. Extraction of the morphometric parameters of the gullies

The parameters used in the study can be divided into two categories, basic parameters and derived parameters, depending on whether they are directly measured from the data sets. The former type includes length, width, and depth, and the sinuosity and slope parameters belong to the latter. In the data sets from HiRISE and ZY-3, both DEMs were derived from the stereo images, and can be naturally matched well with the images. The orthographic image and LiDAR data sets in Meteor crater have been geometrically rectified, and also matched very well. Therefore, we integrated the DEM and orthoimage of each data set in ArcGIS, and extracted typical gullies in vector format from the images. The extracted gullies were then superposed on the DEM data, and the terrain data for the gullies was finally obtained. Fig. 3 shows the implementation of the above method with the corresponding typical cross profiles in the three data sets used in the study.

It is important to note that all the parameters are assigned to the cross profiles of the gullies, as mentioned above. For each typical gully, many transverse profiles were manually sampled from beginning to end with uniform spacing, and points, such as the

Table 1
Summary of the HiRISE data and DTM products used in this study.

Type of terrain	DTM	Resolution (m/pixel)	Latitude (center)	Longitude (center)	HiRISE stereo images
Sand dunes	DTEEC_007018_1255_007229_1255_A01.IMG	0.99	−54.2°	12.93°	PSP_007018_1255 PSP_007229_1255
Terrace	DTEPC_013097_1115_013585_1115_U01.IMG	0.99	−68.4°	1.32°	ESP_013097_1115 ESP_013585_1115
Crater walls	DTEEC_005943_1380_011428_1380_A01.IMG	1.00	−41.5°	202.2°	PSP_005943_1380 ESP_011428_1380
	DTEEC_007110_1325_006820_1325_A01.IMG	0.99	−46.9°	18.79°	PSP_006820_1325 PSP_007110_1325

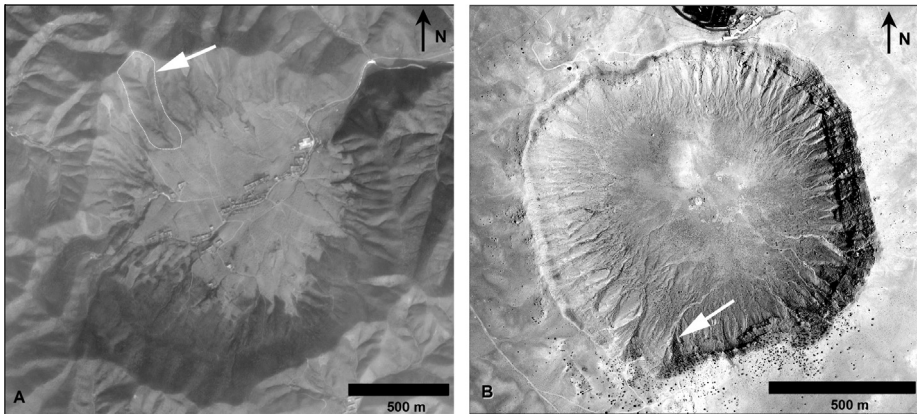

Fig. 2. Example gullies in the walls of the Xiuyan crater (outlined by dashed lines and indicated by the arrow; Nadir image from ZY-3 stereo camera) and Meteor crater (indicated by the arrow; 96592519.tif, orthographic image from the USGS National Map Viewer).

points of inflection transects, were also usually adopted (Fig. 3). The cross profiles of gullies are generally V-shaped, as sketched in Fig. 4, and the two maximum height points (A and B) on the two sides and a deepest point (C) in the channel were first identified. The distance from the lower channel top (A) to the deepest point (C) is defined as the depth d of the gully in cross section, and the width w of the gully refers to the distance between the two maximum height points (A and B). The length $L1$ denotes the distance from each section to the head along the gully, and the overall length L is the sum of all the sections.

We adopted a similar method to that of Mangold et al. (2010) to define the sinuosity index S as the ratio between the channel length ($L1$) and the straight line from the head to each cross-section of the channel ($L0$). We also established two slope parameters, $s1$ and $s2$, to describe the slopes of the gully channel cross sections. These are calculated using the ratio of $d/w1$ and $d'/w2$, as shown in Fig. 4. In addition, we defined the parameter U to be the sum of the left and right slope of the profile. Finally, we established relationships among the above parameters using the method of least squares regression, to give some insights into the formation of gullies' in different geologic settings.

3.2. Uncertainties of morphometric parameters in different data sets

In this study, several data sets with different resolutions were used, and the uncertainties in the derived morphometric parameters of the gullies are also different. All martian gullies and the resulting parameters are calculated based on the DTM from HiRISE stereo images. The vertical precision of the DTM product is usually in the tens of centimeters (http://hirise.lpl.arizona.edu/dtm/about.php), and McEwen et al. (2007) reported that the expected vertical precision of HiRISE DEMs is 0.1–0.2 m. Liu et al. (2012) verified that the vertical accuracy of the DEM products from ZY-3 imagery is 2.2–2.9 m, depending on the influence of the terrain, and the number and distribution of ground control points. The horizontal precision of the above DTMs can be considered as their resolution, given the rigorous photogrammetric models created in both processes. The DEM of Meteor crater was generated from the laser point cloud data, which were acquired using an Optech GEMINI Airborne Laser Terrain Mapper (ALTM) with a vertical accuracy of 0.05–0.30 m (Palucis and McEnulty, 2010). The horizontal accuracy of the DEM can be considered to be the spatial resolution of 1.0 m used in the study, considering that the original laser points were so dense.

With the above accuracies available for each category of data set, we can evaluate the uncertainties of the parameters used in the study. As mentioned in the above section, gullies are first extracted in images and then overlaid on the corresponding DTMs, and an accuracy of 0.5 pixels should be ensured in the DTM, because the image resolution is several times higher than the derived DTM products. In addition, according to the law of error propagation, the parameters for depth (d), width (w), and length (L) should have an accuracy of $\sqrt{2}$ times the above accuracy in extracting the gullies.

A functional relationship for the sinuosity index (S) and slope (s) parameters on the horizontal and vertical scale and can be expressed as:

$$y = f(d, w, L) \tag{1}$$

where f represents the functional relationship and y is the parameter. The accuracies (RMS errors) of y can be derived according to the law of error propagation:

$$\sigma_y = \sqrt{\left(\frac{\partial f}{\partial d}\right)^2 \cdot \sigma_d^2 + \left(\frac{\partial f}{\partial w}\right)^2 \cdot \sigma_w^2 + \left(\frac{\partial f}{\partial L}\right)^2 \cdot \sigma_L^2} \tag{2}$$

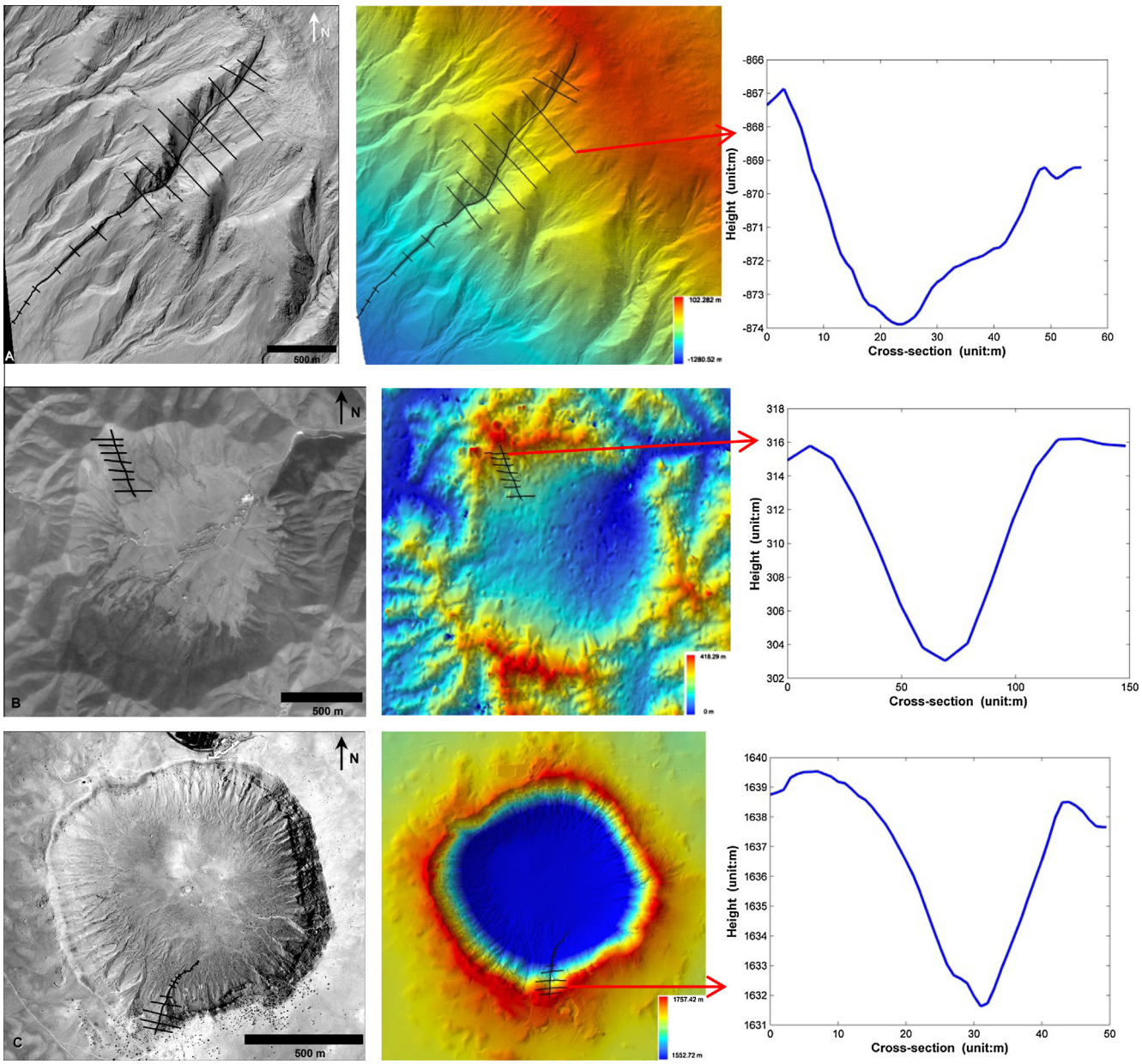

Fig. 3. Process of gully extraction. Gullies were first extracted from images (left column) from HiRISE (A, HiRISE RED channel, subset of PSP_005943_1380), nadir image from ZY-3 stereo camera (B), and orthographic image from the USGS National Map Viewer (C; 96592519.tif). The extracted vectors of gullies are then superposed on the corresponding DEM, and the typical cross profiles, indicated by the arrows, are also shown in the right column.

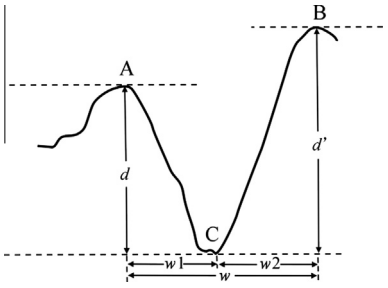

Fig. 4. Definitions of the morphometric parameters of the gullies. See text for details.

Table 2
Accuracies (RMS errors) for the parameters used in the study for all the data sets.

	HiRISE DEM	ZY-3 DEM	LiDAR DEM
L (m)	0.71	7.1	0.71
w (m)	0.71	7.1	0.71
d (m)[a]	0.28	4.10	0.42
s (°)	1.61[b]	2.37	0.78
S	0.0007[b]	0.0179	0.0034

[a] Refers to the maximum accuracies (RMS errors) for each data set.
[b] Refers to the maximum accuracies (RMS errors) among all types of gully for each data set.

The accuracies of the sinuosity index (S) and the slope (s) not only depend on the accuracies of the basic measurements of gullies, but they also are related to the dimensional scales. The mean accuracies for the parameters in all the data sets are evaluated in Table 2, and the basic parameters for all types of gullies are listed in Table 3.

4. Results

We manually extracted unambiguous typical gullies from different data sets. As a result, 10 gullies in martian crater walls, 10 in martian terraces, 12 in martian sand dunes, 5 in the Xiuyan crater wall, and 12 in the Meteor crater wall were selected. Each gully has sufficient cross-sections to statistically describe its morphologies. The statistical results for the lengths (L) of 49 gullies, and other parameters for all the extracted cross profiles with respective RMS errors on the martian surface and the Earth surface are shown in Table 3. The gullies in Xiuyan and Meteor craters are very similar in general, and they are also formed under similar conditions, as verified by the sediments underneath the crater floor (Chen et al., 2010; Kumar et al., 2010). Therefore we combined them together in the subsequent analysis. Of the basic parameters, the lengths of the martian gullies in crater walls, terraces, and sand dunes are similar. All of them are longer than the gullies in the Earth crater walls, which is probably because of small Xiuyan and Meteor craters. The depth and width are the smallest in the sand dunes for all the gullies, which shows that erosion in martian sand dunes is very slight vertically and laterally. The statistics also strongly indicate that all the gullies are very similar in their bilateral slopes and overall sinuosity, which shows that all the gullies have similar morphologies, although their size differs largely.

Fig. 5 shows plots of basic information on the gullies, including the length, depth, and width of each transect profile from each type of gully. In Fig. 5a, the width/length ratio was selected as the ordinate and the length as the abscissa, which removes deviation caused by the scale. On the basis of the same consideration, the logarithmic values of the width were assigned as the abscissa and the depth as the ordinate. In Fig. 5, gullies in sand dunes are always at the bottom, which is consistent with the above analyses, in which they have the smallest width and depth of all the gully categories. However, another important point is that all the gullies seem to follow some distribution, as shown in Fig. 5, which also inspires us to determine the regularities among the gullies.

The possible implicit relationships among these parameters were studied by using the method of least squares regression. Fig. 6 shows that there are good correlations between the width/length ratio and the length for gullies in different geologic settings, and the functional relationships are listed in Table 4. Despite the differences in basic parameters for the gullies, the width/length ratios clearly decrease with length for all gullies, and most importantly, in a similar way. The curve for gullies in sand dunes decreases fastest at approximately 200 m compared to others, which shows that the variation of their widths was heavily depressed henceforth. In the case of Earth craters, the location of the knee point is similar, but in a much more gentle way relative to those in sand dunes, which shows that there is much higher variation in upstream gullies in Earth crater walls than in martian sand dunes. Gullies in martian crater walls and terrace show very similar trends in the relationships between the width/length ratio and the length of gullies, except the depth is relatively smaller in the former case.

Fig. 7 shows the good correlation between depth and width for all the gullies in different geologic settings, and the functional relationships are listed in Table 4. All the depths of the gullies increase with width at a very similar rate (0.10–0.12), while the gullies in sand dunes have exceptionally small dimensions compared to others. The linear relationship between the depth and width could indicate that the erosion abilities increase similarly in the lateral and vertical directions for all the gullies, and the low ratio (0.10–0.12) shows that lateral erosion is about 10 times easier than in vertical direction.

Fig. 8 shows the relationships between depth and U (the summation of two slopes of the cross-sections, in degrees). The functional relationships with the corresponding RMS of fitting and correlation coefficients are listed in Table 4. Gully depth also increases with parameter U, which may indicate that steep channels have also been eroded deeply. The relationship for gullies in sand dunes is linear, and in other cases, a quadratic is much more applicable. This indicates that the depth of linear gullies would increase in a relatively constant way, while in other gullies the depth firstly increase slowly and then very fast after some critical value is exceeded in the slope.

Fig. 9 plots the sinuosity versus length of gullies in different backgrounds, in which the sinuosity indices fall within the scope of 1.0 and 1.2 in all cases. Although positive correlation relationships existed in all the cases, the variation of the sinuosity indices with length is very small and it is particular the truth in the case of martian linear gullies. The functional relationships with the corresponding RMS of fitting and correlation coefficients are also listed in Table 4, in which the extremely small coefficients of the length also indicate that the sinuosity indices are almost constant. The extremely small coefficients of the length also lead to all the correlation coefficients almost 1.0, because the intercepts can essentially represent the linear relationships between sinuosity and length.

Table 3
Statistics of the morphometric parameters of gullies.

		Mars			Earth	
		Crater wall	Terrace	Sand dunes	Xiuyan crater wall	Meteor crater wall
L (km)	Mean	1.56	1.37	2.47	0.61	0.31
	RMS	1.09	0.40	0.29	0.09	0.05
w (m)	Mean	120.83	81.29	9.93	98.70	30.82
	RMS	156.28	78.74	3.73	33.21	28.92
d (m)	Mean	10.11	7.08	0.91	6.78	4.01
	RMS	17.38	9.29	0.75	4.93	4.43
$s1$ (°)	Mean	8.58	9.80	14.36	9.42	16.23
	RMS	6.08	4.76	9.03	5.56	6.35
$s2$ (°)	Mean	8.97	8.90	14.60	10.17	16.49
	RMS	6.85	4.86	8.11	5.42	7.10
S	Mean	1.05	1.03	1.03	1.06	1.05
	RMS	0.04	0.02	0.01	0.02	0.03

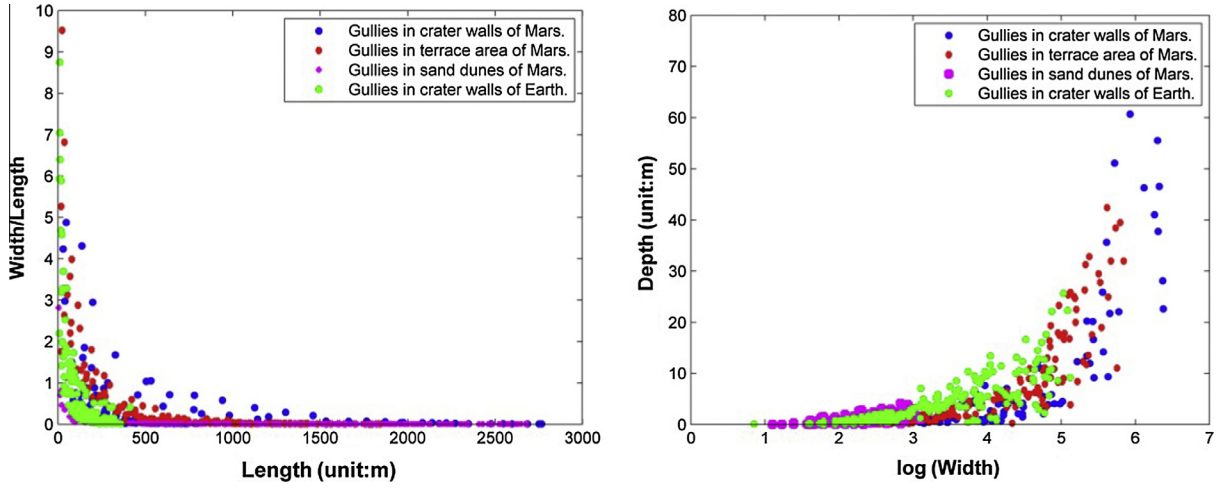

Fig. 5. Length, width, and depth of each gully transect profile. (a) Length versus width/length (left). (b) Width (in logarithmic coordinates) versus depth (right).

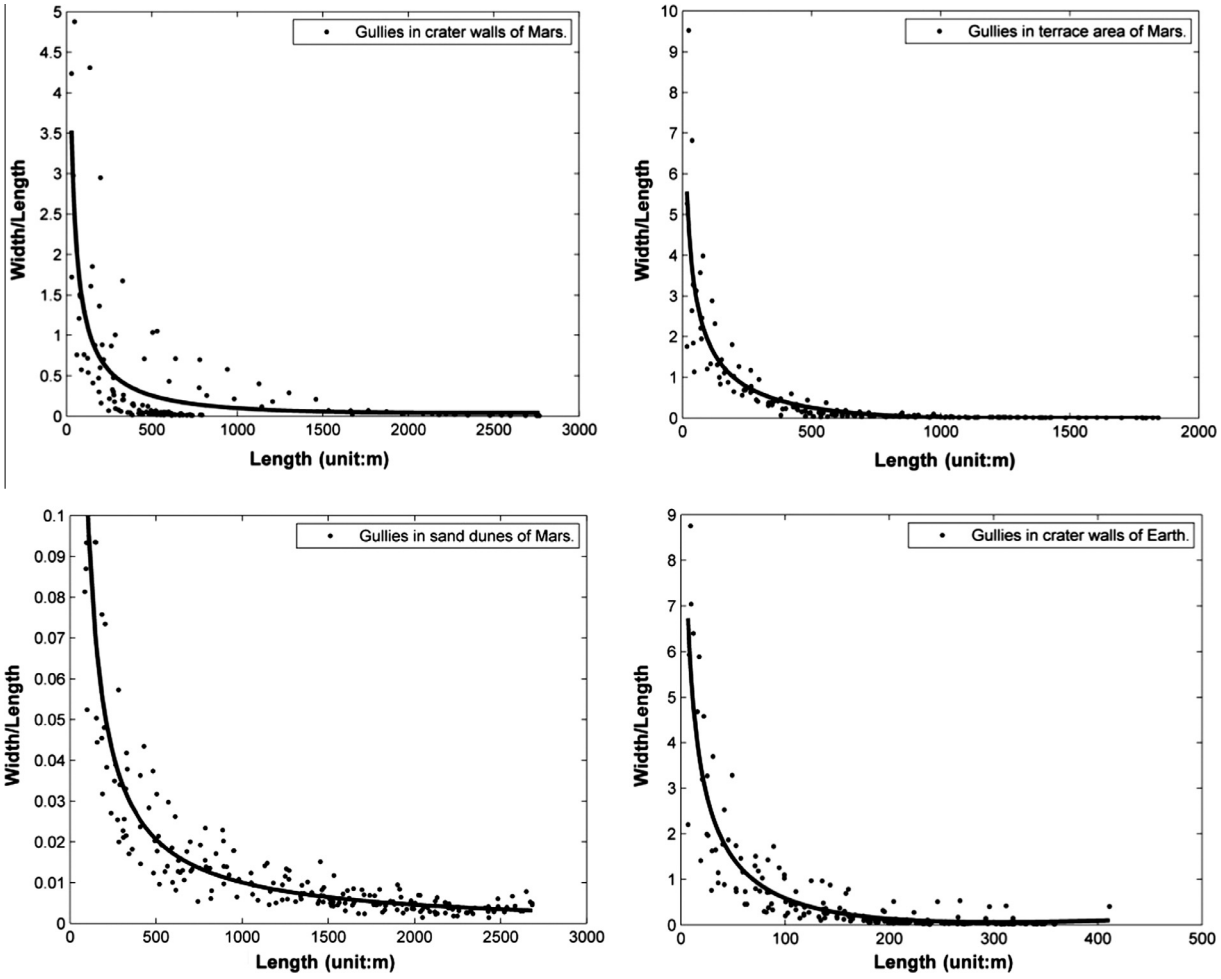

Fig. 6. Relationships between width/length ratio and length for gullies in different geologic settings.

5. Discussion

Morphological characteristics, quantitatively expressed by shape parameters and the inherent relationships, are indications of intrinsic causes, and it is possible to investigate the formation mechanism of gullies by analyzing their morphometric parameters and latent relationships. These specific morphometric techniques have been successfully used in previous terrestrial studies. For example, Fan et al. (2014) recently established regression models for different types of landslides including debris/rock avalanche, debris flow, rock fall, and debris/rock slide by randomly selecting 340 from more than 60,000 landslides induced by Wenchuan

Table 4
Fitting relationships for the morphological parameters of gullies.

Parameters		Fitted relationships	RMS of fitting	Correlation coefficient
Width and length	Gullies in martian crater walls	$w/L = -1.81 + 0.20 \log L + 35.52/L^{0.6}$	0.54	0.74
	Gullies in martian terraces	$w/L = -84.59 + 4.90 \log L + 101.28/L^{0.1}$	0.64	0.85
	Gullies in martian sand dunes	$w/L = 0.003 - 0.0004 \log L + 10.28/L^{1.0}$	0.01	0.99
	Gullies in Earth crater walls	$w/L = -127.42 + 8.11 \log L + 143.67/L^{0.1}$	0.62	0.88
Depth and width	Gullies in martian crater walls	$d = -1.83 + 0.10w$	7.95	0.89
	Gullies in martian terraces	$d = -1.87 + 0.11w$	3.64	0.91
	Gullies in martian sand dunes	$d = -0.30 + 0.12w$	0.59	0.61
	Gullies in Earth crater walls	$d = 0.46 + 0.10w$	2.74	0.80
Depth and U	Gullies in martian crater walls	$d = 0.94 - 0.08\ U + 0.02\ U^2$	13.05	0.66
	Gullies in martian terrace	$d = 1.45 - 0.37U + 0.03\ U^2$	5.08	0.84
	Gullies in martian sand dunes	$d = -0.19 + 0.04U$	0.52	0.72
	Gullies in Earth crater walls	$d = 0.16 + 0.11U + 0.0007\ U^2$	4.23	0.40
Sinuosity and length	Gullies in martian crater walls	$S = 1.0047 + 2.51e{-}5L$	0.02	1.0
	Gullies in martian terraces	$S = 1.0062 + 2.05e{-}5L$	0.01	1.0
	Gullies in martian sand dunes	$S = 1.015 + 6.54e{-}6L$	0.01	1.0
	Gullies in Earth crater walls	$S = 1.0026 + 1.82e{-}4L$	0.05	1.0

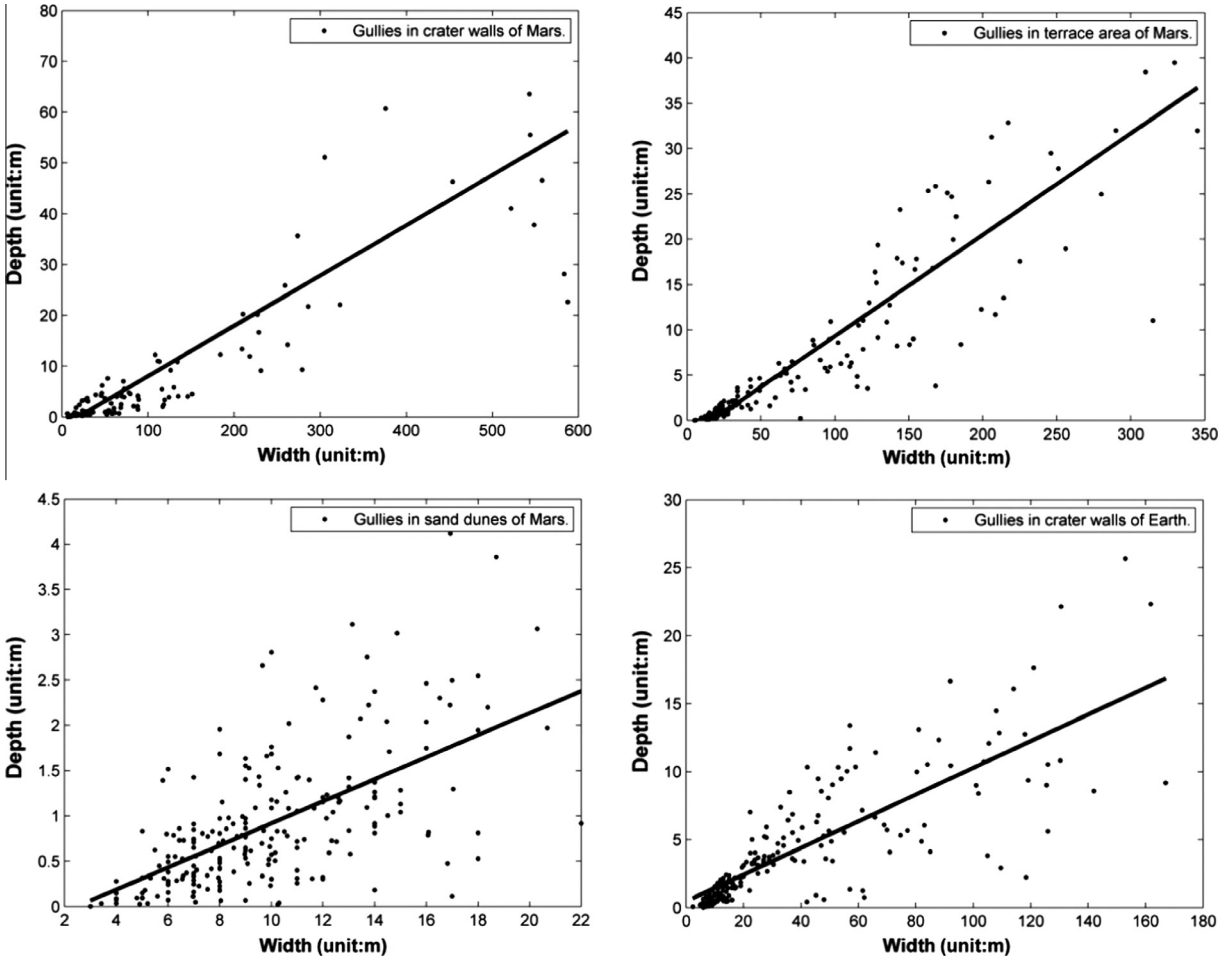

Fig. 7. Relationships between the gully width and length in different geologic settings.

earthquake in China, in which the morphometric parameters of volume, length or runout distance, vertical drop or internal relief of landslides are used. Similarly, Conway et al. (2014) successfully separated the debris flows and fluvial gullies deliberately selected on Earth with a linear combination of morphometric variables such as the slope and concavity, and made a further comparison with martian gullies and finally concluded that martian gullies probably formed by water-driven processes. Soukhovitskaya and Manga (2006) have also successfully discriminated debris flows from dry landslides on Earth by regressing relationships only with the morphometric parameters of volume and length, which were then extended to identify the origination of landslides in Valles Marineris as we have addressed before. However, it is evident that the results of morphometric analysis heavily depend on the

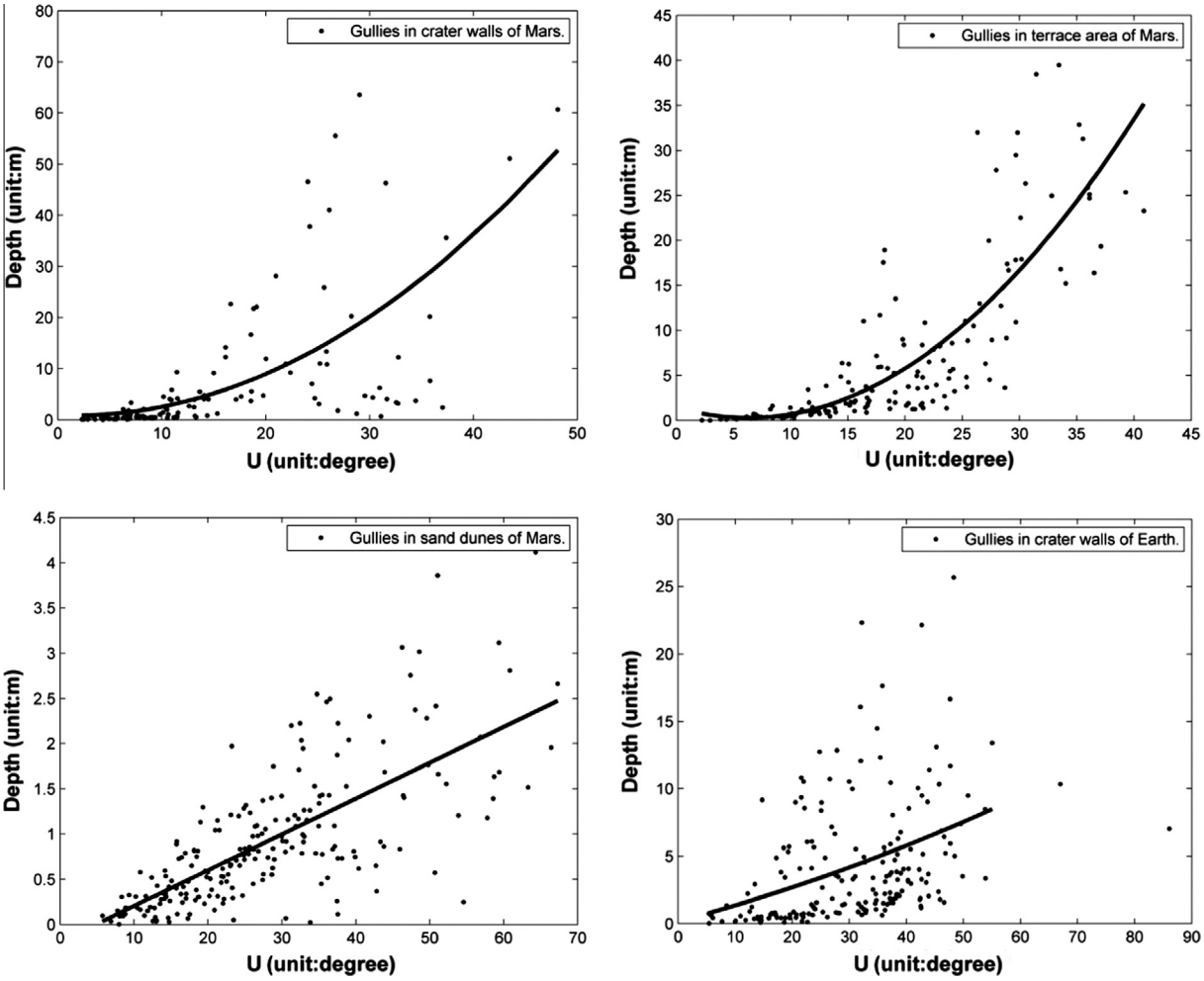

Fig. 8. Relationships between depth and *U* (in degrees) of gullies in different geologic settings.

strategy and the parameter choice, and the specification of the details of gullies can suppress the inadequacy and then contribute to uncovering their origins. Therefore, we adopted the strategy of extracting cross profiles along typical gullies and then obtaining parameters for length, width, depth, and sinuosity for each segment from the head of the gully for each profile, and for the slopes of each cross section. To demonstrate how the parameters change along martian gullies, the parameters of width, depth, sinuosity, and slope were plotted against the scaled length (Fig. 10). The scaled length is the ratio of the distance between current cross section and the gullies' head to gullies' overall length, and it can facilitate comparison between gullies with different magnitudes. Each curve in Fig. 10 represents one gully respectively indicated by the arrow in Fig. 1 under corresponding environment, and it is evident that except linear gully varies slightly in the parameters of width, depth, and sinuosity, other gullies changes dramatically along the gullies. Fig. 10a (up left) is the variation of gullies' width against the scaled length along the gullies, and it clearly shows that width varies along the gully and in the cases of crater walls even up to 10 times. Similar situation appears in the parameter of depth as shown in Fig. 10b (up right), and there are also relatively slight variations in gullies on martian terrace. Fig. 10c (lower left) shows the variation of sinuosity of different gullies, in which gullies in martian terrace are heavily decreased. However, in Fig. 10d (lower right) of cross-section slope, all of them vary greatly along the scaled length. Therefore, variations of the selected shape parameters do exist along all of the gullies, and therefore the strategy of extracting cross profiles along typical gullies by us can better demonstrate the similarities and differences of gullies in different environments than solely assigning one value to each gully. Recently, Narlesky and Gulick (2014) and Hernandez et al. (2014) also adopted the strategy by sampling transects respectively along the length of 17 gullies in the wall of Palikir crater and 12 gullies within Corozal crater, and both of the results supported that a fluvial processes would be more possible for martian gullies origination and some flow characteristics, such as flow velocities and average sediment transport rate, were further estimated based on some shape parameters including slope, concavity, sinuosity, etc.

However, in the research we also made statistics to the parameters based on the whole gully to compare our results with previous work (Table 3). For example, Heldmann et al. (2007) analyzed gullies (mostly exposed on crater walls) from 137 MOC images in the northern hemisphere. The mean gully length obtained (by summing the length of alcove, channel, and apron) was 1.54 km, which is very close to our result of 1.56 km (Table 3). Statistics on the sinuosity index *S* on gullies in martian craters were performed by Mangold et al. (2010) with approximately 3600 individual gully channels in the 250 MOC images, and the results showed that only 3.5% of individual gullies display an index >1.05, which is consistent with our results (Table 3). The mean length of gullies in the same megadune in Russell crater is also 2.5 km (Mangold et al.,

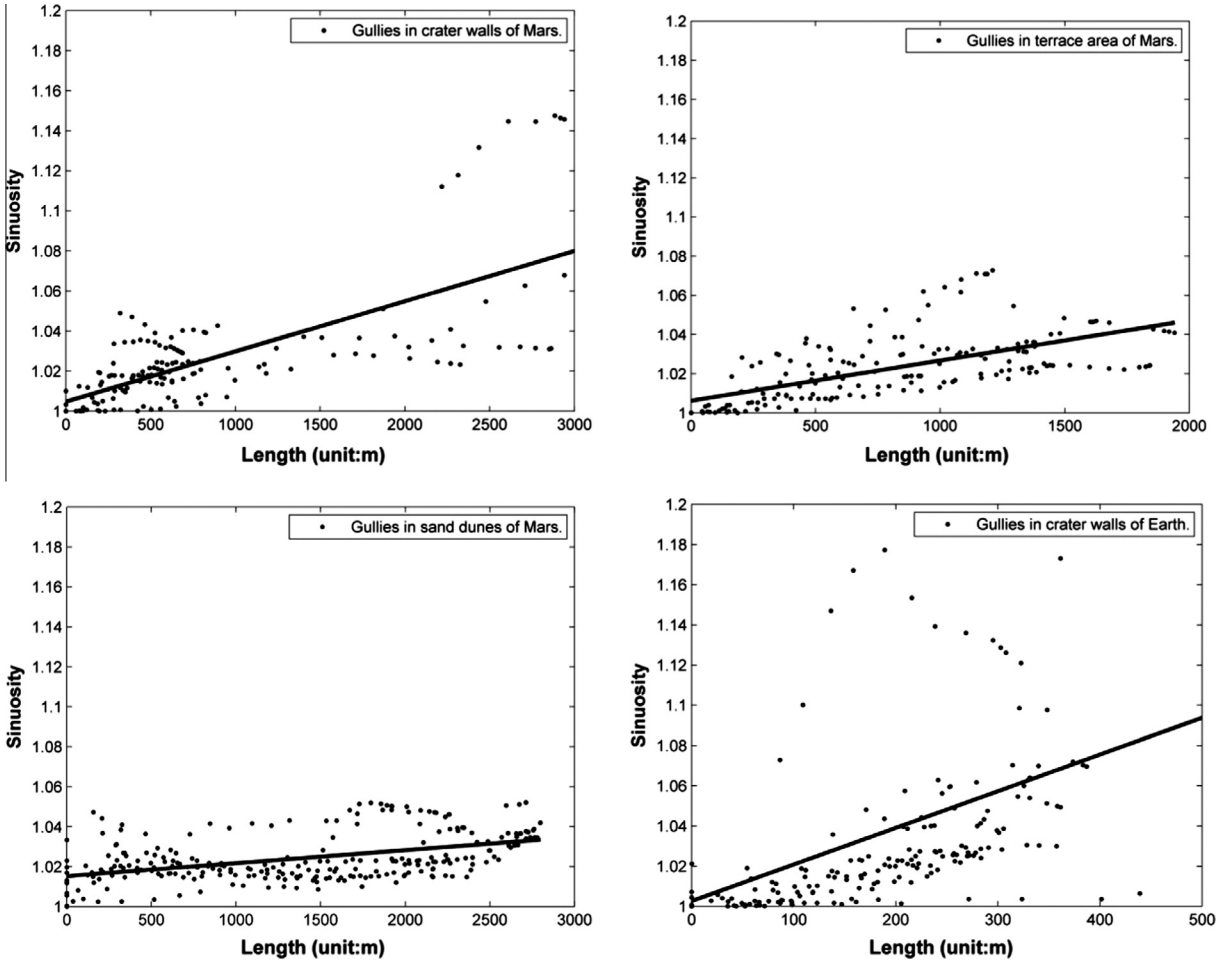

Fig. 9. Relationships between sinuosity and length of gullies in different geologic settings.

2003), which is exactly the same value as in our study. Hobbs et al. (2014) measured classic gullies in Kaiser crater wall, and the mean overall length is about 1.82 km (the value is calculated as the sum of the mean length of the alcove, channel, and apron in their study), slightly larger than our result of 1.56 km, which shows that the size of gullies is dependent on local conditions. However, the sinuosity parameter is highly consistent and equal to 1.03 for both sets of results, indicating that the overall morphology is similar for the linear gullies. The high consistency between our statistics and the previous studies not only proves the effectiveness of our results, but also demonstrates that the gullies extracted in the research are the most representative ones on the martian surface.

Gullies in crater walls on Mars and Earth have similar morphologies except that martian gullies are two to four times larger than their counterparts on Earth, because the latter occur in smaller craters. Their basic morphometric parameters vary greatly, showing that the processes responsible for their formation are complex and easily affected by external factors. Considering the complexity of gully formation in craters on Earth (e.g., pre-existing fractures, rainfall), the formation of gullies in martian craters cannot be attributed to a simple process either. The pre-geologic settings should not be ignored; otherwise it is difficult to explain the phenomenon that most gullies appear in crater walls. The differences in slope and sinuosity between all the gullies are small, showing that their inherent morphologies are similar.

In the research we further explored the possible relationships among the morphometric parameters, in which the ratios between the parameters are used to decrease the influence exerted by the different geologic backgrounds. The relationships between the parameters and the ratios of the cross profiles derived in the study are basically similar, indicating that the processes responsible for their formation created intrinsically similar morphologies. There is a negative correlation between width/length ratio and length for all gullies (Fig. 6), which is interpreted as the erosion ability not increasing significantly down the gullies. If gullies are largely formed by fluid processes, then the fluid should mainly come from the source head (e.g., rainfall in Earth crater walls). The approximately linear dependence between depth and width shown in Fig. 7 indicates that the erosion ability would increase both laterally and vertically, and mere dry mass wasting seems difficult to reconcile with the results. In addition, the positive correlation between the slope and depth further reinforces the above view. The relationships of logarithmic (or exponential), linear, and their combination are probably from the logarithmic correlations of channels' discharge to their dimensions and velocity (Melosh, 2011).

Linear gullies are morphologically much different from those both in Mars and Earth crater walls, which could also be reflected from our morphometric analysis. Linear gullies have the lowest morphological diversities of all the types of gully, which can be seen from the RMS of the length, width, and depth given in Table 3. This morphometric homogeneity could indicate that they were formed by relatively stable process, which should suffer less influence from external factors (e.g., topography). For all gullies, their width and depth increase small or even decrease with gullies' length, indicating the erosion ability of the source agent mainly

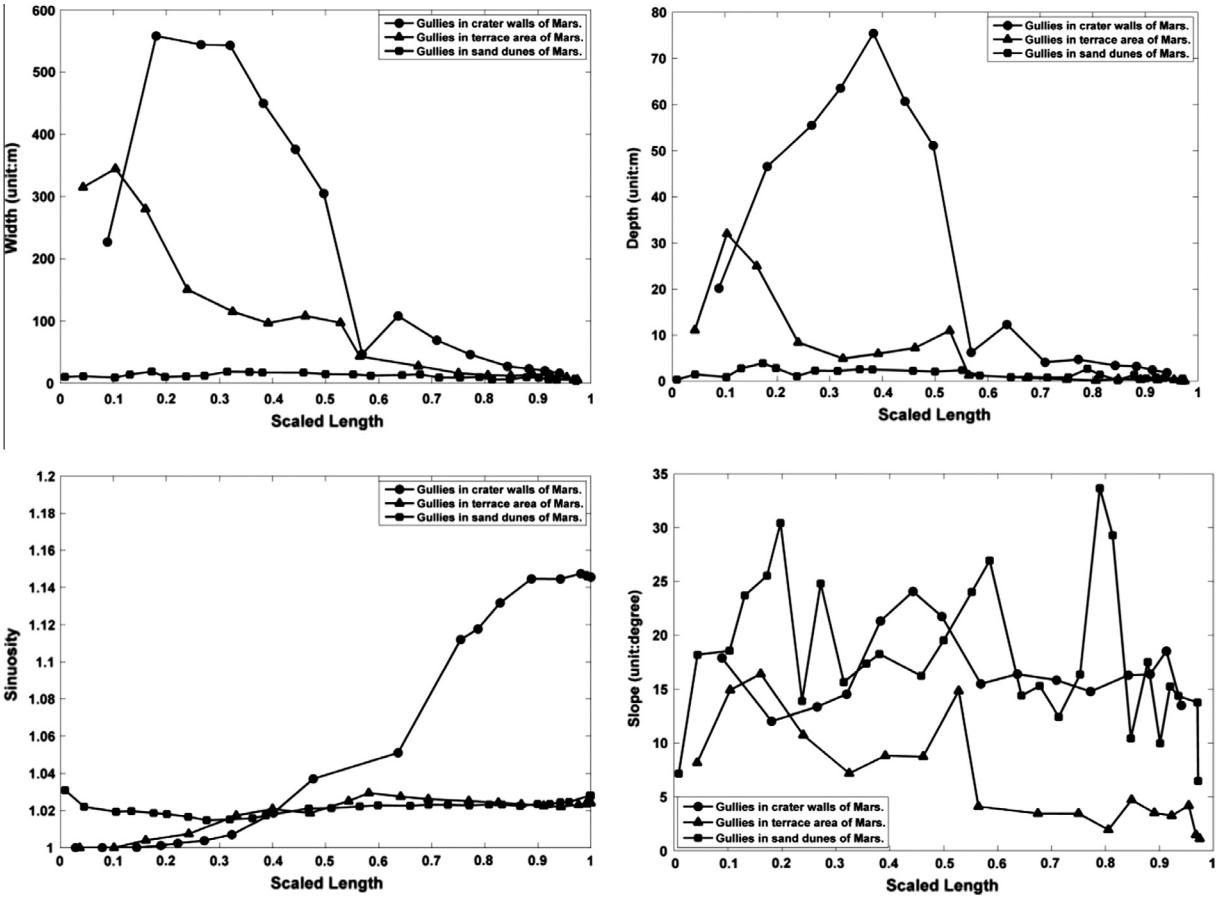

Fig. 10. Variations of width (a), depth (b), sinuosity (c), and slope (d) against the scaled length along typical gullies in different environments. See context for the detail.

comes from the head of gullies. Once initiated, the process would advance at a relatively smooth velocity. In addition, except for the relationships between depth and width, the linear gullies have different correlations among the other parameters and the situation is much more evident in the case of the slope of cross-section and depth. A linear relationship is much more suitable in the case of linear gullies other than a quadratic relationship in other cases. This indicates that the amount of the source agent responsible for the linear gullies is very small that even the skin weak layer of martian surface is not penetrated, while the erosion is strong enough in other cases and the bed rock has been incised to form steep channel. Therefore, although the agents (e.g., surface flow, slippage) responsible for their formation are probably similar, other particular factors, including the differences in lithology and amount of source agent(s), might also play important roles in gullies formation. And the combined result of these factors finally leads to the linear gullies' characteristic of a long channel with limited extension in the vertical and lateral directions. There was a huge controversy on linear gullies formation, from earlier wet mechanism to recent tracks of CO_2 ice blocks, as we have thoroughly reviewed, and the above morphometric results should be considered in future study.

6. Conclusions

We performed quantitative morphological analysis on gullies in martian crater walls, terraces, and sand dunes, and in Earth crater walls. After statistical analysis of the overall characteristics of the gullies in different geologic settings, we further adopted a strategy to extract the parameters of the cross profiles along gullies and established relationships among the parameters using the method of least squares regression. Investigation of the morphometric characteristics of gullies in different settings revealed that

(1) Gullies in different geologic settings are similar in their morphometric parameters and inherent correlations, indicating that similar processes are responsible for their formation. Morphometric differences also show that these processes played different roles in the gullies in different geologic settings.
(2) Morphometric parameters and the relationships of gullies in crater walls on Earth and Mars are extraordinarily similar, except for their magnitudes. Therefore, the processes that occurred in the formation of gullies in Earth crater walls, including surface runoff and dry flows or downslope slumping, as well as the pre-existing geologic structures of impact-related fractures and faults should give insights into the formation of gullies in martian crater walls.
(3) Relative to gullies in crater walls and terraces, linear gullies were formed at a stable velocity, as indicated by their morphometric homogeneity. The constancy of width and depth of gully channels shows that the erosion agents, in combination with the ambient geologic setting, had small ability for undermining and lateral scouring.

Acknowledgments

This study is supported by the National Basic Research Program of China (Project No. 2013CB733201). The authors would like to thank the anonymous reviewers for their constructive and insightful comments.

References

Arfstrom, J.D., 2002. A model of recent martian gully and alcove formation by seepage of water. Lunar Planet. Sci. XXXIII. Abstract #1174.

Balme, M.R. et al., 2006. Orientation and distribution of recent gullies in the southern hemisphere of Mars: Observations from High Resolution Stereo Camera/Mars Express (HRSC/MEX) and Mars Orbiter Camera/Mars Global Surveyor (MOC/MGS) data. J. Geophys. Res. 111, E05001, http://dx.doi.org/10.1029/2005JE002607.

Bleamaster, L.F., Crown, D.A., 2005. Mantle and gully associations along the walls of Dao and Harmakhis Valles, Mars. Geophys. Res. Lett. 32, L20203, http://dx.doi.org/10.1029/2005GL023548.

Bridges, N.T., Lackner, C.N., 2006. Northern hemisphere martian gullies and mantled terrain: Implications for near-surface water migration in Mars' recent past. J. Geophys. Res. 111, E09014, http://dx.doi.org/10.1029/2006JE002702.

Brown, R.B., Holland, D., McKellip, R.D., Navard, A.R., 2008. Creation of high resolution terrain models of Barringer meteorite crater (meteor crater) using photogrammetry and terrestrial laser scanning methods. Lunar Planet. Sci. XXXIX. Abstract #2453.

Chen, M., Xiao, W., Xie, X., Tan, D., Cao, Y., 2010. Xiuyan crater, China: Impact origin confirmed. Chinese Sci. Bull. 55, 1777–1781. http://dx.doi.org/10.1007/s11434-010-3010-1.

Christensen, P.R., 2003. Formation of recent martian gullies through melting of extensive water-rich snow deposits. Nature 422, 45–48. http://dx.doi.org/10.1038/nature01436.

Conway, S.J., Balme, M.R., Murray, J.B., Towner, M.C., 2014. A signal for water on Mars: The comparison of topographic long profiles of gullies on Earth to gullies on Mars. Lunar Planet. Sci. 45. Abstract #2438.

Costard, F., Forget, F., Mangold, N., Peulvast, J.P., 2002. Formation of recent martian debris flows by melting of near-surface ground ice at high obliquity. Science 295, 110–113, http://dx.doi.org/10.1126/science.1066698.

Dickson, J., Head, J., Kreslavsky, M., 2007. Martian gullies in the southern mid-latitudes of Mars: Evidence for climate-controlled formation of young fluvial features based upon local and global topography. Icarus 188, 315–323, http://dx.doi.org/10.1016/j.icarus.2006.11.020.

Diniega, S., Byrne, S., Bridges, N.T., Dundas, C.M., McEwen, A.S., 2010. Seasonality of present-day martian dune-gully activity. Geology 38, 1047–1050, http://dx.doi.org/10.1130/G31287.1.

Diniega, S., Byrne, S., Dundas, C.M., McEwen, A.S., Bridges, N.T., 2011. Present-day martian dune gully formation. Lunar Planet. Sci. XLII. Abstract #1540.

Diniega, S., Hansen, C.J., McElwaine, J.N., Hugenholtz, C.H., Dundas, C.M., McEwen, A.S., Bourke, M.C., 2013. A new dry hypothesis for the formation of martian linear gullies. Icarus 225, 526–537, http://dx.doi.org/10.1016/j.icarus.2013.04.006.

Dundas, C.M., McEwen, A.S., Diniega, S., et al., 2010. New and recent gully activity on Mars as seen by HiRISE. Geophys. Res. Lett. 37, L07202, http://dx.doi.org/10.1029/2009GL041351.

Dundas, C.M., Diniega, S., Hansen, C.J., Byrne, S., McEwen, A.S., 2012. Seasonal activity and morphological changes in martian gullies. Icarus 220, 124–143, http://dx.doi.org/10.1016/j.icarus.2012.04.005.

Fan, X., Rossiter, D.G., van Westen, C.J., Xu, Q., Görüm, T., 2014. Empirical prediction of coseismic landslide dam formation. Earth Surf. Process. Landforms.. http://dx.doi.org/10.1002/esp.3585.

Glines, N.H., Gulick, V.C., 2014. Comparative study of gullies in Kaiser crater on Mars. Lunar Planet. Sci. 45. Abstract #2926.

Haberle, R.M. et al., 2001. On the possibility of liquid water on present-day Mars. J. Geophys. Res. 106, 23317–23326, http://dx.doi.org/10.1029/2000JE001360.

Head, J.W., Marchant, D.R., Kreslavsky, M.A., 2008. Formation of gullies on Mars: link to recent climate history and insolation microenvironments implicate surface water flow origin. Pro. Nat. Acad. Sci. U.S.A. 105, 13258–13263.

Hecht, M.H., 2002. Metastability of liquid water on Mars. Icarus 156, 373–386, http://dx.doi.org/10.1006/icar.2001.6794.

Heldmann, J.L., Mellon, M.T., 2004. Observations of martian gullies and constraints on potential formation mechanisms. Icarus 168, 285–304.

Heldmann, J.L., Carlsson, E., Jonansson, H., Mellon, M.T., Toon, O.B., 2007. Observations of martian gullies and constraints on potential formation mechanisms: II. The northern hemisphere. Icarus 188, 324–344, http://dx.doi.org/10.1016/j.icarus.2006.12.010.

Hernandez, D.J., Gulick, V.C., Narlesky, C.A., 2014. Gullies on Mars: Fluvial geologic processes as evidence for liquid water on Mars. Lunar Planet. Sci. 45. Abstract #1198.

Hobbs, S.W., Paull, D.J., Clarke, J.D.A., 2013. The influence of slope morphology on gullies: Terrestrial gullies in Lake George as analogues for Mars. Planet. Space Sci. 81, 1–17, http://dx.doi.org/10.1016/j.pss.2012.10.009.

Hobbs, S.W., Paull, D.J., Clarke, J.D.A., 2014. A comparison of semiarid and subhumid terrestrial gullies with gullies on Mars: Implications for martian gully erosion. Geomorphology 204, 344–365, http://dx.doi.org/10.1016/j.geomorph.2013.08.018.

Hoffman, N., 2002. Active polar gullies on Mars and the role of carbon dioxide. Astrobiology 2, 313–323. http://dx.doi.org/10.1089/153110702762027899.

Horgan, B., Bell, J., 2012. Seasonally active slipface avalanches in the north polar sand sea of Mars: Evidence for a wind-related origin. Geophys. Res. Lett. 39, L09201. http://dx.doi.org/10.1029/2012GL051329.

Ingersoll, A.P., 1970. Mars: Occurrence of liquid water. Science 168, 972–973. http://dx.doi.org/10.1126/science.168.3934.972.

Kereszturi, A., Mhlmann, D., Berczi, Sz., Ganti, T., Kuti, A., Sik, A., Horvath, A., 2009. Recent rheologic processes on dark polar dunes of Mars: Driven by interfacial water? Icarus 201, 492–503.

Kirk, R.L. et al., 2008. Ultrahigh resolution topographic mapping of Mars with MRO HiRISE stereo images: Meter-scale slopes of candidate Phoenix landing sites. J. Geophys. Res. 113, E00A24, http://dx.doi.org/10.1029/2007JE003000.

Kneissl, T., Reiss, D., van Gasselt, S., Neukum, G., 2010. Distribution and orientation of northern-hemisphere gullies on Mars from the evaluation of HRSC and MOC-NA data. Earth Planet. Sci. Lett. 294, 357–367, http://dx.doi.org/10.1016/j.epsl.2009.05.018.

Kossacki, K.J., Markiewicz, W.J., 2010. Interfacial liquid water on Mars and its potential role in formation of hill and dune gullies. Icarus 210, 83–91. http://dx.doi.org/10.1016/j.icarus.2010.06.029.

Kumar, P.S., Head, J.W., Kring, D.A., 2010. Erosional modification and gully formation at Meteor crater, Arizona: Insights into crater degradation processes on Mars. Icarus 208, 608–620, http://dx.doi.org/10.1016/j.icarus.2010.03.032.

Levy, J.S., Head, J.W., Marchant, D.R., Dickson, J.L., Morgan, G.A., 2009. Geologically recent gully–polygon relationships on Mars: Insights from the Antarctic Dry Valleys on the roles of permafrost, microclimates, and water sources for surface flow. Icarus 201, 113–126, http://dx.doi.org/10.1016/j.icarus.2008.12.043.

Levy, J.S., Head, J.W., Dickson, J.L., Fassett, C.I., Morgan, G.A., Schon, S.C., 2010. Identification of gully debris flow deposits in Protonilus Mensae, Mars: Characterization of a water-bearing, energetic gully-forming process. Earth Planet. Sci. Lett. 294, 368–377, http://dx.doi.org/10.1016/j.epsl.2009.08.002.

Liu, B., Sun, X., Di, K., Liu, Z., 2012. Accuracy analysis and validation of ZY-3's sensor corrected products. Rem. Sens. Land Resour. 24, 36–40 (in Chinese with English abstract).

Lobitz, B., Wood, B.L., Averner, M.M., McKay, C.P., 2001. Use of spacecraft data to derive regions on Mars where liquid water would be stable. Proc. Nat. Acad. Sci. U.S.A. 98, 2132–2137.

Malin, M.C., Edgett, K.S., 2000. Evidence for recent groundwater seepage and surface runoff on Mars. Science 288, 2330–2335. http://dx.doi.org/10.1126/science.288.5475.2330.

Mangold, N., Costard, F., Forget, F., 2003. Debris flows over sand dunes on Mars: Evidence for liquid water. J. Geophys. Res. 108, 5027, http://dx.doi.org/10.1029/2002JE001958.

Mangold, N. et al., 2010. Sinuous gullies on Mars: Frequency, distribution, and implications for flow properties. J. Geophys. Res. 115, E11001, http://dx.doi.org/10.1029/2009JE003540.

McEwen, A.S. et al., 2007. Mars reconnaissance orbiter's High Resolution Imaging Science Experiment (HiRISE). J. Geophys. Res. 112, E05S02, http://dx.doi.org/10.1029/2005JE002605.

Mellon, M.T., Phillips, R.J., 2001. Recent gullies on Mars and the source of liquid water. J. Geophys. Res. 106, 23165–23180, http://dx.doi.org/10.1029/2000JE001424.

Melosh, H.J., 2011. Planetary Surface Processes. Cambridge Planetary Science, New York, p. 410.

Mischna, M.A., Richardson, M.I., Wilson, R.J., McCleese, D.J., 2003. On the orbital forcing of martian water and CO_2 cycles: A general circulation model study with simplified volatile schemes. J. Geophys. Res. Planets 108 (E6). http://dx.doi.org/10.1029/2003JE002051.5062.

Miyamoto, H., Dohm, J.M., Baker, V.R., Beyer, R.A., Bourke, M., 2004. Dynamics of unusual debris flows on martian sand dunes. Geophys. Res. Lett. 31, L13701, http://dx.doi.org/10.1029/2004GL020313.

Moehlmann, D., 2008. The influence of van der Waals forces on the state of water in the shallow subsurface of Mars. Icarus 195, 131–139.

Musselwhite, D.S., Swindle, T.D., Lunine, J.I., 2001. Liquid CO_2 breakout and the formation of recent small gullies on Mars. Geophys. Res. Lett. 28, 1283–1285, http://dx.doi.org/10.1029/2000GL012496.

Narlesky, C.A., Gulick, V.C., 2014. Geomorphic and flow analysis for gullies in Palikir crater. Lunar Planet. Sci. 45. Abstract #2870.

Palucis, M., McEnulty, T., 2010. Meteor crater, Az: A Terrestrial Analog to Study Gully Formation on Mars, Mapping Project Report <http://www.lpi.usra.edu/publications/books/barringer_crater_guidebook/LiDAR/NCALM_mapping_project.pdf>.

Pelletier, J.D., Kolb, K.J., McEwen, A.S., Kirk, R.L., 2008. Recent bright gully deposits on Mars: wet or dry flow? Geology 36, 211–214.

Reiss, D., Jaumann, R., 2003. Recent debris flows on Mars: Seasonal observations of the Russell crater dune field. Geophys. Res. Lett. 30, 1321, http://dx.doi.org/10.1029/2002GL016704.

Reiss, D., van Gasselt, S., Neukum, G., Jaumann, R., 2004. Absolute dune ages and implications for the time of formation of gullies in Nirgal Vallis, Mars. J. Geophys. Res. 109, E06007, http://dx.doi.org/10.1029/2004JE002251..

Reiss, D., Erkeling, G., Bauch, K.E., Hiesinger, H., 2010. Evidence for present day gully activity on the Russell crater dune field, Mars. Geophys. Res. Lett. 37, L06203, http://dx.doi.org/10.1029/2009GL042192..

Reiss, D., Hauber, E., Hiesinger, H., et al., 2011. Terrestrial gullies and debris-flow tracks on Svalbard as planetary analogs for Mars. Geol. Soc. Am. Spec. Pap. 483, 165–175. http://dx.doi.org/10.1130/2011.2483(11).

Schon, S.C., Head, J.W., Fassett, C.I., 2009. Unique chronostratigraphic marker in depositional fan stratigraphy on Mars: Evidence for ca. 1.25 Ma gully activity and surficial meltwater origin. Geology 37, 207–210, http://dx.doi.org/10.1130/G25398A.1.

Soukhovitskaya, V., Manga, M., 2006. Martian landslides in Valles Marineris: Wet or dry? Icarus 180, 348–352, http://dx.doi.org/10.1016/j.icarus.2005.09.008.

Tang, X. et al., 2012. Triple linear-array imaging geometry model of Ziyuan-3 surveying satellite and its validation. Acta Geodaet. Cartograph. Sinica 41, 191–198 (in Chinese with English abstract).

Treiman, A.H., 2003. Geologic settings of martian gullies: Implications for their origins. J. Geophys. Res. 108, 8031–8042, http://dx.doi.org/10.1029/2002JE001900.

Védie, E., Costard, F., Font, M., Lagarde, J.L., 2008. Laboratory simulations of martian gullies on sand dunes. Geophys. Res. Lett. 35, L21501, http://dx.doi.org/10.1029/2008GL035638.

Wang, X., Luo, L., Guo, H., et al., 2013. Cratering process and morphological features of the Xiuyan impact crater in Northeast China. Sci. China Earth Sci. 56, 1629–1638. http://dx.doi.org/10.1007/s11430-013-4695-1.

Williams, K., Toon, O., Heldmann, J., McKay, C., Mellon, M., 2008. Stability of mid-latitude snowpacks on Mars. Icarus 33, 565–577.